Plasmonic fractals: ultrabroadband light trapping in thin film solar cells by a Sierpinski nanocarpet

Hanif Kazerooni[1], Amin Khavasi,[2,*]

1. Chemical Engineering Faculty, Amirkabir University of Technology (Tehran Polytechnic), Tehran, Iran

2. Electrical Engineering Department, Sharif University of Technology, P.O. Box: 11155-4363 Tehran, Iran

Corresponding author: khavasi@sharif.edu

Abstract

Plasmonic Sierpinski nanocarpet as back structure for a thin film Si solar cell is investigated. We demonstrate that ultra-broadband light trapping can be obtained by placing square metallic nanoridges with Sierpinski pattern on the back contact of the thin film solar cell. The multiple-scale plasmonic fractal structure allows excitation of localized surface plasmons and surface plasmon polaritons in multiple wavelengths leading to obvious absorption enhancements in a wide frequency range. Full wave simulations show that 109% increase of the short-circuit current density for a 200 nm thick solar cell, is achievable by the proposed fractal back structure. The amount of light absorbed in the active region of this cell is more than that of a flat cell with semiconductor thickness of 1000 nm.

Keywords: Plasmonics, Fractals, Light trapping, Thin film photovoltaic

1. Introduction

Thin film photovoltaic cells potentially have a lower cost compared to the conventional wafer-based cells [1, 2]. However, in thin film cells most of the incident light is not absorbed, in particular, for the indirect-bandgap semiconductor Si [3]. Therefore, light trapping structures have to be used to increase the absorptance.

A new method for absorption enhancement in thin film solar cells is the use of metallic nanostructures [2-7]. Metallic-dielectric interfaces support surface plasmon polaritons (SPP), electromagnetic waves propagating along the interface. The incident light can be coupled to these waves and also photonic modes of the structure by using periodic metallic structures [3]. So the optical path, and consequently the absorption inside the semiconductor are significantly increased. Another mechanism for absorption enhancement in plasmonic solar cells, is the coupling of the light to localized surface plasmons (LSP) which leads to the strong local field enhancement around the metal nanoparticles. The near field enhancement increase absorption in a surrounding semiconductor material. The nanoparticles then act as an effective 'antenna' for the incident light [3]. However, significant absorption enhancement is usually occurred in a relatively narrow frequency range; since these modes (i.e. LSP and SPP) are excited at a specific wavelength, the enhancement at other wavelengths is inconsiderable.

It is demonstrated that fractals are promising structures to achieve broadband electromagnetic responses [8-13]. Fractal is an object replicates itself on successively smaller scales [14]. This multiple-scale property of fractal geometries leads to broadband spectral response [8] and similar behavior in multiple wavelengths which is useful in broadband application such as multiband antennas [15], extraordinary transmission in multiple wavelengths [9, 16], and multiple photonic band gaps [10].

In this work, we combine the wideband response of fractal geometries with the idea of surface-plasmon-assisted absorption enhancement by using metallic gratings, to obtain broadband light trapping in a thin film Si solar cell. In particular, we focus on a well-known fractal geometry, namely the Sierpinski carpet. Considerable absorption enhancement in a wide frequency range is achieved by using the proposed structure. We demonstrate by full wave simulations that metallic back structure with Sierpinski carpet pattern of square nanoridges attached to a thin-film solar cell can significantly increase the short-circuit current density. The full wave simulations are performed using CST Microwave Studio [17].

2. Plasmonic Sierpinski back structure

Fig. 1 shows the construction of the Sierpinski carpet for the back structure of cell, it starts with a metallic square of side length d (Fig. 1(a)). This square is then divided into a grid of 3×3, d/3-sided squares and a square metallic ridge is placed on the central sub-square (Fig. 1(b)). The same procedure is then recursively applied to the remaining 8 squares. We stop the procedure at the second level (Fig. 1(c)), because dimensions of the ridges are so small at upper levels that they are difficultly realizable with current fabrication techniques.
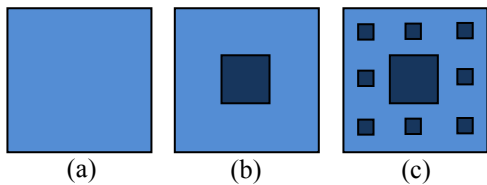

Figure 1. Sierpinski carpet: (a) zeroth, (b) first and (c) second fractal levels.
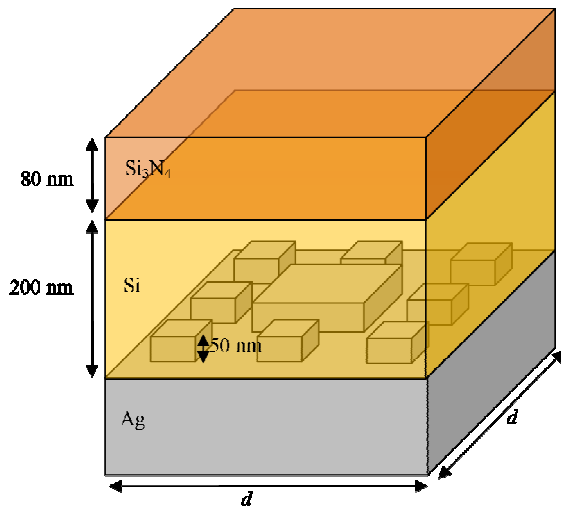
Figure 2. One period of the silicon solar cell under study. Silver square nanoridges on the back contact construct a second order Sierpinski carpet.

One period of the cell under study is illustrated in Fig. 2 which is consist of a back structure made of Ag, a Si layer with 200 nm thickness and a standard antireflection coating made of Si_3N_4 whose thickness is 80 nm. Square silver nanoridges whose heights are 50 nm, with second order Sierpinski pattern are placed on the Ag back contact of the structure. The Drude model is assumed for dielectric function of Ag with $\varepsilon_\infty = 3.7$, plasma frequency $\omega_p = 1.38 \times 10^{16}$ rad/s, and collision frequency $\gamma = 2.73 \times 10^{13}$ 1/s which is an excellent fit to experimental results [18]. The refractive index of Si_3N_4 is taken to be $n = 2$, and the refractive index of Si is taken from [19].

3. Results

The absorption $A(\lambda)$ of the structure whose period is set to $d = 350$ nm, under normal incidence versus wavelength λ of the incident wave is plotted in Fig. 3. Zeroth order, first order and second order Sierpinski fractals are used on the Ag back contact of the cell and their corresponding absorptions are depicted with dotted red, dashed green and solid blue lines, respectively. The relation $A(\lambda) = 1 - R(\lambda)$ is used for computing the absorption in this simulation, where $R(\lambda)$ is the ratio of reflected power to the incident power at each wavelength. It is clearly seen that when $\lambda > 500$ nm, the absorption is significantly enhanced, especially for second order fractal. Interestingly, over a wide wavelength range (500 nm$< \lambda <$750 nm) the absorption is almost complete. It has been already demonstrated that the absorption enhancement is due to the coupling of light to the plasmonic mode propagating at the interface of semiconductor and metal [4], however, the enhancement achieved in previous works was narrowband. The broadband absorption enhancement obtained here can be attributed to the different length scales of Sierpinski carpet that enables coupling of light at different wavelengths to the plasmonic modes.

It should be noted that in short wavelengths (smaller than 500 nm) the silicon layer act as a thick optical layer for the light. Therefore the light cannot interact with the nanostructure at the back of the film. This would be the reason that most of the absorption enhancement occurs for wavelengths more than 500 nm in Fig. 3.
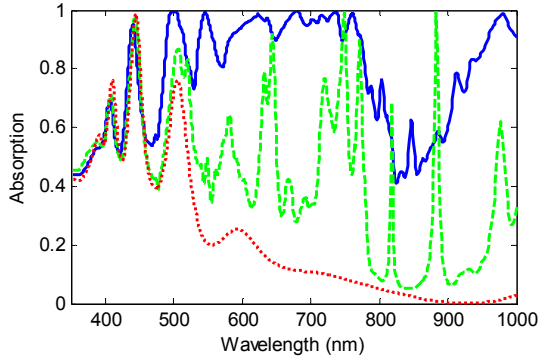
Figure 3. Absorption spectra for the Si solar cell with zeroth order (dotted red), first order (dashed green) and second order (solid blue) Sierpinski fractal on its back contact.

Next, we calculate N_A/N_I which is defined here as the ratio of absorbed photons in the structure to the incident photons for solar spectrum (AM1.5G). This parameter is obtained by using the following equation:

$$\frac{N_A}{N_I} = \frac{\frac{1}{hc}\int S(\lambda)A(\lambda)\lambda d\lambda}{\frac{1}{hc}\int S(\lambda)\lambda d\lambda} \tag{1}$$

where h is the Plank constant, c is the light speed and $S(\lambda)$ is the incident solar power density. Figure 4 shows calculated N_A/N_I when the period is varied from 200 nm to 450 nm, it is seen that for $d = 350$ nm the ratio of absorbed photons is maximized. It is worth noticing that the solar cell with second order fractal back structure can absorb more than half (58% for $d = 350$ nm) of the incident photons while this ratio is less than 14% for the reference simple cell (zeroth order fractal).
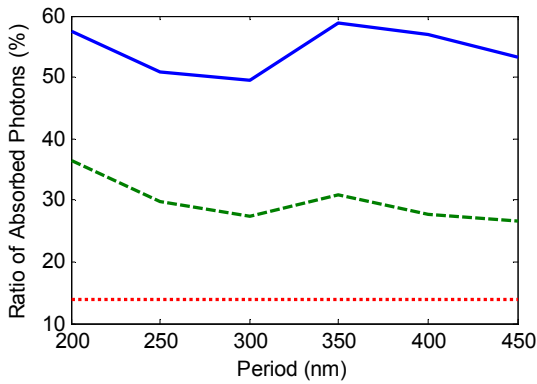

Figure 4- Ratio of absorbed photons versus the structure period for the Si solar cell with zeroth order (dotted red), first order (dashed green) and second order (solid blue) Sierpinski fractal on its back contact.

It should be emphasized that only the photons absorbed in the semiconductor contribute to photo-current and those absorbed in the metallic back contact are lost. The absorption power density in each layer can be calculated from the divergence of the Poynting vector [20]:

$$P_{abs} = \frac{1}{2}\omega\varepsilon''|E|^2 + \frac{1}{2}\omega\mu''|H|^2 \qquad\qquad (2)$$

where ω is the frequency, ε'' is the imaginary part of the permittivity, E is the electric field, μ'' is the imaginary part of the permeability, and H is the magnetic field. For most materials, $\mu'' = 0$ and the second term drops out. Figure 5(a) shows the absorption spectra in each layer for the reference cell with flat back contact. It is obvious from this figure that the absorption in metallic layer is negligible. Because the incident light cannot couple to the SPP mode and this is due to the momentum mismatch between the incident light and the SPP mode. On the other hand, as it is illustrated in Fig. 5(b), in the case of the cell with the proposed second order Sierpinski fractal on its back contact, significant part of the incident wave with $\lambda > 500$ nm is lost in the metallic region. This is due to the fact that in this range the main mechanism for absorption is the coupling of incident wave to the plasmonic modes, and it has been shown that these modes at the Ag/Si interface suffers high plasmon losses [3]. However, the absorption of the proposed fractal cell is still much higher than that of the reference flat cell.

We calculate the short-circuit current density to compare the performance of the proposed fractal cell with the reference cell. The short-circuit current density is given by

$$J_{sc} = \frac{e}{hc}\int \eta_c S(\lambda) A_{Si}(\lambda)\lambda d\lambda \qquad\qquad (3)$$

where e is the electron charge, A_{Si} is the absorption in the Si layer and η_c is the collection efficiency [4]. For simplicity the collection efficiency of Si material is assumed here to be a constant of 80%, which means that 80% of the incident light would be absorbed to generate electron-hole pairs. With these assumptions and by using equation (3), the estimated short-circuit current density for the reference flat cell and the cell with the proposed second order fractal back structure are 6.61 (mA/cm^2) and 13.83 (mA/cm^2), respectively. This means that using fractal back structure enhances the short-circuit current by 109% compared with the solar cell with flat back contact. The enhancement will be 67% if the first order fractal is used.
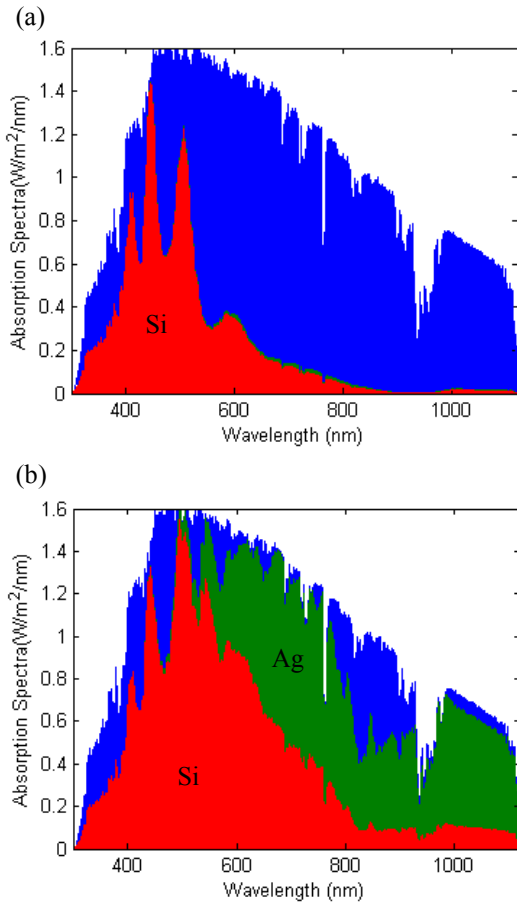
(a)

(b)

Figure 5- Incident solar spectrum (AM1.5G) (blue) and calculated absorption spectra in silicon layer (red) and silver back contact (green) for (a) the reference cell with flat back contact (zeroth order fractal) and (b) the proposed cell with second order fractal on its back contact.

4. Conclusion

In summary, we have proposed a novel light trapping scheme by using plasmonic Sierpinski nanocarpet on the back structure of thin film solar cells. As a proof of concept, a Si thin film cell has been investigated. It has been shown that a back structure made of square nanoridges whose geometry resembles second order Sierpinski carpet can enhance the short-circuit current density by 109% compared with a cell with a flat back contact. The proposed fractal structure may be used for efficient light trapping in other thin film technologies as well as organic solar cells.

It is worth mentioning that the amount of light absorbed in the 200 nm thick Si layer of the proposed structure with fractal geometry is even higher than that of a flat cell with 1000 nm thick Si layer. Therefore, by using fractal geometry the cell thickness can be substantially reduced and the thickness reduction translates into lower production cost, better collection efficiency and higher open-circuit voltage.

References

1. M. A. Green (2002) Third generation photovoltaics: solar cells for 2020 and beyond, Physica E: Low-dimensional Systems and Nanostructures 14:65-70.

2. V. E. Ferry, J. N. Munday, and H. A. Atwater (2010) Design considerations for plasmonic photovoltaics. Advanced Materials 22:4794-4808.

3. H. A. Atwater, and A. Polman (2010) Plasmonics for improved photovoltaic devices. Nat Mater 9:205-213.

4. W. Bai, Q. Gan, F. Bartoli, J. Zhang, L. Cai, Y. Huang, and G. Song (2009) Design of plasmonic back structures for efficiency enhancement of thin-film amorphous Si solar cells. Optics letters 34:3725-3727.

5. K. R. Catchpole, and A. Polman (2008) Plasmonic solar cells. Optics express 16:21793-21800.

6. K. Q. Le, A. Abass, B. Maes, P. Bienstman, and A. Alù (2012) Comparing plasmonic and dielectric gratings for absorption enhancement in thin-film organic solar cells. Optics express 20:A39-A50.

7. R. A. Pala, J. White, E. Barnard, J. Liu, and M. L. Brongersma (2009) Design of Plasmonic Thin-Film Solar Cells with Broadband Absorption Enhancements. Advanced Materials 21:3504-3509.

8. G. Volpe, and R. Quidant (2011) Fractal plasmonics: subdiffraction focusing and broadband spectral response by a Sierpinski nanocarpet. Optics Express 19:3612-3618.

9. Y. J. Bao, B. Zhang, Z. Wu, J. W. Si, M. Wang, R. W. Peng, X. Lu, J. Shao, Z. Li, and X. P. Hao (2007) Surface-plasmon-enhanced transmission through metallic film perforated with fractal-featured aperture array. Applied physics letters 90:251914-251914.

10. W. Wen, L. Zhou, J. Li, W. Ge, C. T. Chan, and P. Sheng (2002) Subwavelength photonic band gaps from planar fractals. Physical review letters 89:223901-4.

11. X. Huang, D. Ye, S. Xiao, J. Huangfu, Z. Wang, L. Ran, and L. Zhou (2009) Fractal plasmonic metamaterials for subwavelength imaging arXiv preprint arXiv:0908.0201.

12. F. Miyamaru, Y. Saito, M. W. Takeda, B. Hou, L. Liu, W. Wen, and P. Sheng (2008) Terahertz electric response of fractal metamaterial structures. Physical Review B 77:045124-6.

13. L. Zhou, W. Wen, C. T. Chan, and P. Sheng (2003) Reflectivity of planar metallic fractal patterns Applied physics letters 82:1012-1014.

14. M. Segev, M. Soljačić, and J. M. Dudley (2012) Fractal optics and beyond Nature Photonics 6:209-210.

15. D. H. Werner, and S. Ganguly (2003) An overview of fractal antenna engineering research. Antennas and Propagation Magazine, IEEE 45:38-57.

16. L. Lan-Ju, J. I. N. Biao-Bing, Z. Qiu-Yi, W. U. Jing-Bo, B. A. O. Yong-Jun, J. I. A. Tao, J. I. A. Xiao-Qing, C. A. O. Chun-Hai, K. Lin, and X. U. Wei-Wei (2012) Extraordinary Transmission through Fractal-Featured Metallic and Superconducting Films at Terahertz Frequency. Chinese Physics Letters 29:114101-4.

17. "www.cst.com (2011 CST Computer Simulation Technology AG).".

18. Johnson, P. B., and Christy, R. W. (1972). Optical constants of the noble metals. Physical Review B 6: 4370-4379.

19.   E. D. Palik, *Handbook of optical constants of solids* (Academic press, 1998).

20.   V. E. Ferry, A. Polman, and H. A. Atwater (2011) Modeling light trapping in nanostructured solar cells. ACS nano 5:10055-10064.